

Polarized Parton Densities in the Nucleon

Elliot Leader

Department of Physics

Birkbeck College, University of London

Malet Street, London WC1E 7HX, England

E-mail: e.leader@physics.bbk.ac.uk

Aleksander V. Sidorov

Bogoliubov Theoretical Laboratory

Joint Institute for Nuclear Research

141980 Dubna, Russia

E-mail: sidorov@thsun1.jinr.dubna.su

Dimiter B. Stamenov

Institute for Nuclear Research and Nuclear Energy

Bulgarian Academy of Sciences

Blvd. Tsarigradsko Chaussee 72, Sofia 1784, Bulgaria

E-mail: stamenov@inrne.acad.bg

Abstract

We present a critical assessment of what can be learnt from the present data on inclusive polarized DIS. We examine critically some of the simplifying assumptions made in recent analyses and study in detail the question of the determination of the gluon, strange sea and valence quark polarized densities.

We have also carried out a new NLO QCD analysis of the world data. We find an excellent fit to the data and present our results for the polarized parton densities.

1. Introduction.

Deep inelastic scattering (DIS) of leptons on nucleons has remained the prime source of our understanding of the internal partonic structure of the nucleon and one of the key areas for the testing of perturbative QCD. Decades of experiments on unpolarized targets have led to a rather precise determination of the unpolarized parton densities. Spurred on by the famous EMC experiment [1] at CERN in 1988, there has been a huge growth of interest in polarized DIS experiments which yield more refined information about the partonic structure. Many experiments have been carried out at SLAC [2]-[6] and CERN [7]-[10] on proton, deuterium and ^3He targets, and there are major programmes under way at SLAC (E155), DESY (HERMES [11]) and CERN (COMPASS).

In addition to the unpolarized structure functions $F_1(x, Q^2)$ and $F_2(x, Q^2)$ there are two independent spin structure functions $g_1(x, Q^2)$ and $g_2(x, Q^2)$ and their unambiguous determination requires measurement of both the longitudinal asymmetry A_{\parallel} and the transverse asymmetry A_{\perp} obtained with a target polarized parallel or perpendicular to the lepton beam direction, respectively. In the recent years there has been a great improvement in the quality of the data on the structure function $g_1(x, Q^2)$, obtained from measurements using a longitudinally polarized target, and a big extension in the kinematic range x and Q^2 covered. Moreover it has become possible to present data in bins of (x, Q^2) rather than simply averaged over Q^2 at each x . The spin dependent structure function $g_2(x, Q^2)$ has now also been extracted [2, 5, 12] from the data although with limited statistical precision compared to the g_1 determination.

The data at very small x has taught us that extrapolation of the measured values to $x = 0$ is a subtle matter, so that the moments of the structure functions should not be considered as genuinely experimental quantities.

Experiments on unpolarized DIS provide information on the unpolarized quark densities $q(x, Q^2)$ and gluon density $G(x, Q^2)$ inside a nucleon. Measurements of $g_1(x, Q^2)$ give us more detailed information, namely the number densities of quarks $q(x, Q^2)_{\pm}$ and gluons $G(x, Q^2)_{\pm}$ whose helicity is respectively along or opposite to the helicity of the parent nucleon. The usual densities are

$$q(x, Q^2) = q_+(x, Q^2) + q_-(x, Q^2) , \quad G(x, Q^2) = G_+(x, Q^2) + G_-(x, Q^2) \quad (1)$$

and the new information is then contained in the polarized structure function $g_1(x, Q^2)$

which is expressed in terms of the *polarized* parton densities

$$\Delta q(x, Q^2) = q_+(x, Q^2) - q_-(x, Q^2) , \quad \Delta G(x, Q^2) = G_+(x, Q^2) - G_-(x, Q^2) . \quad (2)$$

Several theoretical analyses [13] - [21] based on the NLO perturbative QCD calculations [22] have sought to pin down the polarized parton densities. Each of them utilized the different data sets available at the time the analyses were performed. Only in the analyses [16, 19, 20] is essentially all the present data used, the exception being the very recent final E143 results [5]). And none have completely used the information contained in the more detailed binning of the data in (x, Q^2) . Moreover, there are differences in the assumptions to aid the analysis, differences in the choice of the renormalization scheme and differences in the form of the input parton densities and the value Q_0^2 at which they are determined. And finally, there are still significant disagreements about the results. To quote one example, Altarelli et al. [16] have obtained a significant polarized gluon density $\Delta G(x, Q^2)$, whereas Bourrely et al. [21] claim that a perfectly acceptable fit can be obtained with $\Delta G(x, Q^2) = 0$.

Our aim in this paper is twofold:

i) We discuss what can be learnt from the data, in theory and in practice, and examine the role played by the various assumptions used in the theoretical analyses.

ii) We carry out a new study of the world polarized data. In addition to the data used in our previous analysis [18] the more accurate SLAC/E154 neutron data [6], the new more precise SMC proton data [10] which do not indicate a rise of g_1 at small x , the HERMES data [11] and the final data results [5] of the E143 Collaboration at SLAC are now included. In trying to extract as well as possible the polarized parton densities we pay special attention to the observed scaling violations in the A_1 data and use all the information contained in the more detailed binning of them in (x, Q^2) . As in our previous work we use the following parametrization for the input polarized parton densities:

$$\Delta q(x, Q_0^2) = f(x)q(x, Q_0^2) , \quad (3)$$

in which we now utilize the *new* MRST set of unpolarized densities $q(x, Q_0^2)$ [23]. These parton densities account for the new, more precise H1 and ZEUS deep inelastic scattering data, for the re-analysis of the CCFR neutrino data, for the inclusive prompt photon and large E_T jet production in proton-proton collisions and for the charge asymmetry in Drell-Yan reactions. The MRST analysis leads to a value $\alpha_s(M_z^2) = 0.1175$ in excellent agreement with the world average $\alpha_s(M_z^2) = 0.118 \pm 0.005$ [24].

2. Ambiguities and subtleties in determining the polarized parton densities

There are several difficulties, specific to the polarized case, which make it much harder than in the unpolarized case to obtain reliable and unambiguous information about the polarized densities.

2.1. What can be deduced in principle

In the unpolarized case the separation of the contributions from partons of different flavours relies heavily upon the existence of both charged current neutrino and neutral current electromagnetic data. At present, and for some years to come, the information from polarized inelastic measurements will be limited to neutral current data. This raises the interesting question as to what one can hope to learn, both in theory and in practice.

We have available data on $g_1^{(p)}(x, Q^2)$ and $g_1^{(n)}(x, Q^2)$ (or $g_1^{(d)}(x, Q^2)$) structure functions expressed as linear combinations of either the individual parton densities

$$\Delta u + \Delta \bar{u}, \quad \Delta d + \Delta \bar{d}, \quad \Delta s + \Delta \bar{s} \quad (4)$$

and ΔG or, equivalently, the $SU(3)$ flavour combinations

$$\begin{aligned} \Delta q_3 &= (\Delta u + \Delta \bar{u}) - (\Delta d + \Delta \bar{d}) , \\ \Delta q_8 &= (\Delta u + \Delta \bar{u}) + (\Delta d + \Delta \bar{d}) - 2(\Delta s + \Delta \bar{s}) , \\ \Delta \Sigma &= (\Delta u + \Delta \bar{u}) + (\Delta d + \Delta \bar{d}) + (\Delta s + \Delta \bar{s}) \end{aligned} \quad (5)$$

and ΔG . (Note that Δq_8 is defined in such a way that its first moment is $\sqrt{3}$ times the expectation value of the eighth component of the Cabibbo axial vector $SU(3)$ current.)

We are trying therefore to obtain information about four functions of x and Q^2 on the basis of experimental data on the two independent functions $g_1^{(p)}(x, Q^2)$ and $g_1^{(n)}(x, Q^2)$. It is simpler to discuss the situation in terms of the contributions Δq_3 , Δq_8 , $\Delta \Sigma$ and ΔG .

We have

$$g_1^{p(n)}(x, Q^2) = \frac{1}{2} \left(\frac{2}{9} \right) \{ \delta C_{NS} \otimes [\pm \frac{3}{4} \Delta q_3 + \frac{1}{4} \Delta q_8] + \delta C_S \otimes \Delta \Sigma + \delta C_G \otimes \Delta G \} , \quad (6)$$

where δC_{NS} , δC_S and δC_G are the non-singlet, singlet and gluon Wilson coefficient functions, respectively. In (6) \otimes denotes convolution with respect to x and $2/9$ is the average value of the charge squared $\langle e^2 \rangle$ when the number of flavours $N_f = 3$.

Note that taking into account more than 3 active flavours does not change the main conclusions in this and the next section.

Let us firstly suppose that we have perfect data for a range of x and Q^2 , and that we try to determine the functions Δq_3 , Δq_8 , $\Delta\Sigma$ and ΔG . Then Δq_3 is determined uniquely and trivially since

$$g_1^p(x, Q^2) - g_1^n(x, Q^2) = \frac{1}{6} \delta C_{NS} \otimes \Delta q_3 \quad (7)$$

We are then left with

$$g_1^p(x, Q^2) + g_1^n(x, Q^2) = \frac{2}{9} \left[\frac{1}{4} \delta C_{NS} \otimes \Delta q_8 + \delta C_S \otimes \Delta\Sigma + \delta C_G \otimes \Delta G \right]. \quad (8)$$

It is the difference in the Q^2 -evolution of the three terms on the RHS of (8) that enables them to be determined separately. Indeed, by studying the first and higher derivatives of the LHS of (8) with respect to Q^2 at $Q^2 = Q_0^2$, and using the evolution equations, one can prove that Δq_8 , $\Delta\Sigma$ and ΔG are uniquely determined at $Q^2 = Q_0^2$.

It is immediately clear, given the limited range of Q^2 available and the fact that the data are *not* perfect and have errors, that the separation of Δq_8 , $\Delta\Sigma$ and ΔG from each other will not be very clearcut. Nonetheless, *in principle*, the data fix Δq_3 , Δq_8 , $\Delta\Sigma$ and ΔG or, equivalently, via (4), $\Delta u + \Delta\bar{u}$, $\Delta d + \Delta\bar{d}$, $\Delta s + \Delta\bar{s} \equiv 2\Delta\bar{s}$ and ΔG . But any hope of a successful analysis will depend upon finding simple enough parametrizations of these quantities at $Q^2 = Q_0^2$.

2.2. Valence and sea

It is clear from the above that the inclusive (electromagnetic current) data give no information about the valence parts Δq_v of the quark densities. It is of interest, however, to know the Δq_v and $\Delta\bar{q}$ or equivalently, Δq and $\Delta\bar{q}$, since they play a distinctive role in other types of experiment, e.g. polarized semi-inclusive DIS, polarized Drell-Yan reactions etc. Indeed, an attempt has been made to extract the polarized valence densities from the semi-inclusive data [25], but the quality of the present data precludes an accurate determination of these densities. It is therefore important to make a combined analysis [26] of both the semi-inclusive and inclusive DIS data.

Further, for the unpolarized densities simple parametrizations are normally given for the valence and sea quark densities. One reason for this is that one expects q_v and

\bar{q} to have simple, but very different, behaviours as $x \rightarrow 0$, and this feature is lost when dealing with q or $q + \bar{q}$.

There is some point, therefore, in wanting to deal directly with the valence and sea densities and to this end it has been common practice to make some model assumptions about the polarized sea [13, 14] and [17]- [21], which then allows a determination of the valence parts. For example, the apparently innocuous assumption of a flavour independent polarized sea

$$\Delta\bar{s} = \Delta\bar{u} = \Delta\bar{d} \quad (9)$$

implies that Δu_v and Δd_v are determined, since the data fix $\Delta\bar{s}$, $\Delta u_v + 2\Delta\bar{u}$ and $\Delta d_v + 2\Delta\bar{d}$.

We believe it is important to study the consequences of assumptions like Eq. (9). Consider therefore the family of assumptions at $Q^2 = Q_0^2$

$$\Delta\bar{u} = \Delta\bar{d} = \lambda\Delta\bar{s} , \quad (10)$$

where λ is a parameter.

Given that the data fix $\Delta q_{3,8}$, $\Delta\Sigma$ and ΔG and that

$$\Delta\bar{s} = \frac{1}{6}(\Delta\Sigma - \Delta q_8) , \quad (11)$$

we see that the result for $\Delta\bar{s}$ should not change as λ is varied. This provides a serious test for the stability of the analysis.

Further the dependence of the valence densities upon λ is given by

$$\begin{aligned} \Delta u_v &= \frac{1}{2}[\Delta q_3 + \Delta q_8 - 4(\lambda - 1)\Delta\bar{s}] , \\ \Delta d_v &= \frac{1}{2}[-\Delta q_3 + \Delta q_8 - 4(\lambda - 1)\Delta\bar{s}] , \end{aligned} \quad (12)$$

so that they are sensitive to the assumption about the sea. On the other hand, if the analysis is correct, neither $\Delta q_{3,8}$ nor $\Delta\Sigma(\Delta\bar{s})$ nor ΔG should change as λ is varied.

It should be noticed that Eqs. (10) and (12) are only valid at $Q^2 = Q_0^2$. The equality (10) and therefore Eq. (12) will be (marginally) broken because of the different NLO evolution of the different sea quarks for $Q^2 > Q_0^2$.

It has sometimes been claimed in the literature [19] that as a result of the fits the sea always turns out to be flavour symmetric. Clearly, from the above, one can learn absolutely nothing from the data about $\Delta\bar{u}$ and $\Delta\bar{d}$ and any χ^2 dependence on λ must be an artifact of the fitting procedure.

2.3. Simplifying assumptions

In order to limit the number of parameters being fitted, it is always necessary to take simple functional forms for the parton densities, and sometimes additional simplifying assumptions are made. We have already discussed in the previous section the assumptions regarding the sea quarks (see Eqs. (9) and (10)) widely used in the literature. Another somewhat arbitrary one (for its more recent use see Altarelli et al. [16]), is to assume that

$$\Delta q_3(x, Q^2) = C \Delta q_8(x, Q^2) , \quad (13)$$

where C is a constant.

This is, of course, perfectly compatible with the evolution equations, decreases substantially the number of parameters being fitted, but has no physical justification at all. This assumption leads to a better determination of the rest of the independent parton densities, but it is not clear whether the values and errors of the parameters are not thereby distorted. It is important to check to what extent (13) is compatible with the results of other theoretical analyses of the data in which this approximation is not used.

2.4. Scheme dependence

It is well known that at NLO and beyond, the parton densities become dependent upon the renormalization (or factorization) scheme. In the unpolarized case the most commonly used are the \overline{MS} , MS and DIS schemes and parton densities in different schemes differ from each other by terms of order $\alpha_s(Q^2)$, which goes to zero as Q^2 increases.

There are two significant differences in the polarized case:

i) The singlet densities $\Delta\Sigma(x, Q^2)$, in two different schemes, will differ by terms of order

$$\alpha_s(Q^2)\Delta G(x, Q^2) , \quad (14)$$

which appear to be of order α_s . But it is known [27, 28] that, as a consequence of the axial anomaly, the first moment

$$\int_0^1 dx \Delta G(x, Q^2) \propto [\alpha_s(Q^2)]^{-1} , \quad (15)$$

grows in such a way with Q^2 as to compensate for the factor $\alpha_s(Q^2)$ in (14). Thus the difference between $\Delta\Sigma$ in different schemes is only apparently of order $\alpha_s(Q^2)$, and could be quite large.

ii) Because of ambiguities in handling the renormalization of operators involving γ_5 in n dimensions, the specification \overline{MS} does *not* define a unique scheme. Really there is a family of \overline{MS} schemes which, strictly, should carry sub-label indicating how γ_5 is handled. What is now conventionally called \overline{MS} is in fact the scheme due to Vogelsang and Mertig and van Neerven [22], in which the first moment of the non-singlet densities is conserved, i.e. is independent of Q^2 , corresponding to the conservation of the non-singlet axial-vector Cabibbo currents.

Although mathematically correct it is a peculiarity of this factorization scheme that certain soft contributions are included in the Wilson coefficient functions, rather than being absorbed completely into the parton densities. As a consequence, the first moment of $\Delta\Sigma$ is not conserved so that it is difficult to know how to compare the DIS results on $\Delta\Sigma$ with the results from constituent quark models at low Q^2 .

To avoid these idiosyncrasies Ball, Forte and Ridolfi [15] introduced what they called the AB scheme, which involves a minimal modifications of the \overline{MS} scheme, and for which

$$\begin{aligned}\Delta\Sigma(x, Q^2)_{AB} &= \Delta\Sigma(x, Q^2)_{\overline{MS}} + N_f \frac{\alpha_s(Q^2)}{2\pi} \int_x^1 \frac{dy}{y} \Delta G(y, Q^2)_{\overline{MS}}, \\ \Delta G(x, Q^2)_{AB} &= \Delta G(x, Q^2)_{\overline{MS}}\end{aligned}\tag{16}$$

or, in the Mellin n -moment space,

$$\begin{aligned}\Delta\Sigma(n, Q^2)_{AB} &= \Delta\Sigma(n, Q^2)_{\overline{MS}} + N_f \frac{\alpha_s(Q^2)}{2\pi n} \Delta G(n, Q^2)_{\overline{MS}}, \\ \Delta G(n, Q^2)_{AB} &= \Delta G(n, Q^2)_{\overline{MS}}.\end{aligned}\tag{17}$$

That $\Delta\Sigma(n = 1)_{AB}$ is independent of Q^2 to all orders follows from the Adler-Bardeen theorem [29].

The singlet part of the first moment of the structure function g_1

$$\Gamma_1^{(s)}(Q^2) \equiv \int_0^1 dx g_1^{(s)}(x, Q^2)\tag{18}$$

then depends on $\Delta\Sigma$ and ΔG only in the combination

$$a_0(Q^2) = \Delta\Sigma(1, Q^2)_{\overline{MS}} = \Delta\Sigma(1)_{AB} - N_f \frac{\alpha_s(Q^2)}{2\pi} \Delta G(1, Q^2)\tag{19}$$

and the unexpectedly small value for the axial charge a_0 found by the EMC [1], which triggered the "spin crisis in the parton model" [30], can be nicely explained as due to a cancellation between a reasonably sized $\Delta\Sigma(1)$ and the gluon contribution. Of importance for such an explanation are both the positive sign and the large value (of

order $\mathcal{O}(1)$) for the first moment of the polarized gluon density $\Delta G(1, Q^2)$ at *small* $Q^2 \sim 1 - 10 \text{ GeV}^2$. Note that what follows from QCD is that $|\Delta G(1, Q^2)|$ grows with Q^2 (see Eq. (15)) but its value at *small* Q^2 is unknown in the theory at present and has to be determined from experiment.

Although the AB scheme corrects the most glaring weakness of the \overline{MS} scheme, it does not consistently put all hard effects into the coefficient functions. As pointed out in [31] one can define a family of schemes labelled by a parameter a :

$$\begin{pmatrix} \Delta\Sigma \\ \Delta G \end{pmatrix}_a = \begin{pmatrix} \Delta\Sigma \\ \Delta G \end{pmatrix}_{\overline{MS}} + \frac{\alpha_s}{2\pi} \begin{pmatrix} 0 & z^{(a)}_{qG} \\ 0 & 0 \end{pmatrix} \otimes \begin{pmatrix} \Delta\Sigma \\ \Delta G \end{pmatrix}_{\overline{MS}} \quad (20)$$

where

$$z_{qG}(x; a) = N_f[(2x - 1)(a - 1) + 2(1 - x)] , \quad (21)$$

in all of which (19) holds, but which differ in their expression for the higher moments. (The AB scheme corresponds to taking $a = 2$).

Amongst these we believe there are compelling reasons to choose what we shall call the JET scheme ($a = 1$), i.e.

$$z_{qG}^{JET} = 2N_f(1 - x) . \quad (22)$$

This is the scheme originally suggested by Carlitz, Collins and Mueller [28] and also advocated by Anselmino, Efremov and Leader [32].[†] In it all hard effects are absorbed into the coefficient functions. In this scheme the gluon coefficient function is exactly the one that would appear in the cross section for

$$pp \rightarrow jet(\mathbf{k}_T) + jet(-\mathbf{k}_T) + X , \quad (23)$$

i.e., the production of two jets with large transverse momentum \mathbf{k}_T and $-\mathbf{k}_T$, respectively.

More recently Müller and Teryaev [33] have advanced rigorous and compelling arguments, based upon a generalization of the axial anomaly to bilocal operators, that removal of all anomaly effects from the quark densities leads to the JET scheme. Also a different argument by Cheng [34] leads to the same conclusion. (Cheng calls the JET scheme a chirally invariant (CI) scheme.)

The transformation from the \overline{MS} scheme of Mertig, van Neerven and Vogeslang to the JET scheme is given in moment space by

$$\Delta\Sigma(n, Q^2)_{JET} = \Delta\Sigma(n, Q^2)_{\overline{MS}} + 2N_f \frac{\alpha_s(Q^2)}{2\pi n(n+1)} \Delta G(n, Q^2)_{\overline{MS}} ,$$

[†]There is misprint in Eq. (8.2.6) of [32]. The term $\ln(\frac{1-x/x'}{x/x'})$ should be $[\ln(\frac{1-x/x'}{x/x'}) - 1]$.

$$\Delta G(n, Q^2)_{JET} = \Delta G(n, Q^2)_{\overline{MS}} . \quad (24)$$

Of course, (17) and (24) become the same for $n = 1$.

In this paper we carry out the fitting procedure in the \overline{MS} scheme and the results can then be transformed to the other schemes via (16) and (24). However it will be important to carry out the fitting *in the other schemes* as a check on the stability of the whole analysis [35].

3. Method of analysis and input parton distributions

The spin dependent structure function of interest, $g_1^N(x, Q^2)$, is a linear combination of the asymmetries A_{\parallel}^N and A_{\perp}^N (or the related virtual photon-nucleon asymmetries $A_{1,2}^N$) measured with the target polarized longitudinally or perpendicular to the lepton beam, respectively. Neglecting as usual the subdominant contributions (see for example [8]), $A_1^N(x, Q^2)$ can be expressed *via* the polarized structure function $g_1^N(x, Q^2)$ as

$$A_1^N(x, Q^2) \cong (1 + \gamma^2) \frac{g_1^N(x, Q^2)}{F_1^N(x, Q^2)} = \frac{g_1^N(x, Q^2)}{F_2^N(x, Q^2)} [2x(1 + R^N(x, Q^2))] , \quad (25)$$

where

$$R^N + 1 = (1 + \gamma^2) F_2^N / 2x F_1^N \quad (26)$$

and F_1^N and F_2^N are the unpolarized structure functions. In (25) the kinematic factor γ^2 is given by

$$\gamma^2 = \frac{4M_N^2 x^2}{Q^2} . \quad (27)$$

It should be noted that in the SLAC kinematic region γ cannot be neglected.

In some cases the theoretical analyses of the data are presented in terms of $g_1^N(x, Q^2)$ as extracted from the measured values of $A_1^N(x, Q^2)$ according to (25), using various parametrizations of the experimental data for F_2 and R .

As in our previous analysis we follow the approach first used in [14], in which the next-to-leading (NLO) QCD predictions for the spin-asymmetry $A_1^N(x, Q^2)$ are confronted with the data on $A_1^N(x, Q^2)$, rather than with the $g_1^N(x, Q^2)$ derived by the procedure mentioned above. The choice of A_1^N should minimize the higher twist contributions which are expected to partly cancel in the ratio (25), allowing use of data at lower Q^2 . Bearing in mind that in polarized DIS most of the small x data points are at low Q^2 , a lower than usual cut is needed ($Q^2 > 1 \text{ GeV}^2$) in order to have enough data for the theoretical analysis. We believe that in this approach such a low

Q^2 -cut is more justified.

In NLO approximation

$$A_1^N(x, Q^2)_{NLO} \cong (1 + \gamma^2) \frac{g_1^N(x, Q^2)_{NLO}}{F_1^N(x, Q^2)_{NLO}} . \quad (28)$$

In (28) $N = p$, n and $d = (p + n)/2$.

To calculate $A_1^N(x, Q^2)_{NLO}$ in NLO QCD and then fit the data we follow the same procedure described in detail in our paper [18]. Here we will recall only the main points.

The Q^2 evolution, in NLO QCD approximation, is carried out for the n-space moments of the polarized quark and gluon densities. Then using the known NLO expressions for the moments of the Wilson coefficients $\delta C_q(n, \alpha_s)$ and $\delta C_G(n, \alpha_s)$ (see e.g. [14]) one can calculate the moments of the structure function

$$M^N(n, Q^2) = \frac{1}{2} \sum_q^{N_f} e_q^2 \left[\delta C_q(n) (\Delta q(n, Q^2) + \Delta \bar{q}(n, Q^2)) + \frac{1}{N_f} \delta C_G(n) \Delta G(n, Q^2) \right] . \quad (29)$$

As already mentioned above, all calculations are performed in the \overline{MS} scheme. To account for heavy quark contributions we use the so-called fixed-flavour scheme [36, 14] and set the number of active flavours in (29) $N_f = 3$. In contrast to our previous analysis [18], we now use for the values of the QCD parameter $\Lambda_{\overline{MS}}$: $\Lambda_{\overline{MS}}(n_f = 3) = 353 \text{ MeV}$ and $\Lambda_{\overline{MS}}(n_f = 4) = 300 \text{ MeV}$, which correspond to $\alpha_s(M_z^2) = 0.1175$, as obtained by the MRST analysis [23] of the world unpolarized data, in excellent agreement with the world average $\alpha_s(M_z^2) = 0.118 \pm 0.005$ [24].

Finally, to reconstruct the spin structure functions $g_1^N(x, Q^2)$ in Bjorken x-space from their moments (29) with the required accuracy, we use the Jacobi reconstruction method [37, 38]. Note that in this method the structure functions are given analytically.

The same procedure has been used to calculate the unpolarized structure functions $F_1^N(x, Q^2)_{NLO}$ from their moments.

We choose the input polarized densities at $Q_0^2 = 1 \text{ GeV}^2$ in the form:

$$\begin{aligned} x \Delta u_v(x, Q_0^2) &= \eta_u A_u x^{a_u} x u_v(x, Q_0^2) , \\ x \Delta d_v(x, Q_0^2) &= \eta_d A_d x^{a_d} x d_v(x, Q_0^2) , \\ x \Delta Sea(x, Q_0^2) &= \eta_S A_S x^{a_S} x Sea(x, Q_0^2) , \\ x \Delta G(x, Q_0^2) &= \eta_g A_g x^{a_g} x G(x, Q_0^2) \end{aligned} \quad (30)$$

where on R.H.S. of (30) we have used the MRST unpolarized densities [23].

Guiding arguments for such an ansatz are simplicity (not too many free parameters) and the expectation that polarized and unpolarized densities have similar behaviour at large x . In (30) the parameters α_f account for the difference of the low- x behaviour between the polarized and unpolarized parton densities. The normalization factors A_f are determined in such a way as to ensure that the first moments of the polarized densities are given by η_f .

In the previous section we explained why we chose to deal with valence and sea quarks instead of their singlet and non-singlet combinations. For the polarized light and strange sea quark densities at $Q_0^2 = 1 \text{ GeV}^2$ we adopt the assumption (10). Then

$$\Delta\bar{s} \equiv \Delta\bar{q} = \frac{\Delta Sea}{2(2\lambda + 1)} , \quad \eta_{\bar{s}} = \frac{\eta_S}{2(2\lambda + 1)} , \quad (31)$$

where $\eta_{\bar{s}}$ is the first moment of the strange sea parton density $\Delta\bar{s}$.

We would like to emphasize once more that in contrast to the valence quark densities, $\Delta\bar{s}$ should not depend on the flavour sea decomposition, i.e. on λ in our case (see Eq. (11)), and as will be seen below, our numerical results confirm this.

The first moments of the valence quark densities η_u and η_d are fixed by the octet hyperon β decay constants [39]

$$g_A = F + D = 1.2573 \pm 0.0028, \quad a_8 = 3F - D = 0.579 \pm 0.025 . \quad (32)$$

to be

$$\eta_u = 0.918 - 2(\lambda - 1)\Delta\bar{s}(1, Q_0^2), \quad \eta_d = -0.339 - 2(\lambda - 1)\Delta\bar{s}(1, Q_0^2). \quad (33)$$

In the case of SU(3) flavour symmetry of the sea ($\lambda = 1$) we take

$$\eta_u = 0.918 , \quad \eta_d = -0.339 . \quad (34)$$

The rest of the parameters in (30)

$$\{a_u, a_d, \eta_S, a_S, \eta_g, a_g\} , \quad (35)$$

have to be determined from the best fit to the $A_1^N(x, Q^2)$ data.

In some papers [16, 21] g_A , and in others (see e.g. [17]) both g_A and a_8 have been taken to be free parameters determined by the best fit to the inclusive polarized DIS data. We do not favour such an approach because the values of these quantities, especially g_A , are determined from much more precise experiments and using them improves

the accuracy with which we can determine the polarized densities.

Results of Analysis

In this section we present the results of our fits to the present experimental data on $A_1^N(x, Q^2)$: EMC proton data [1], SLAC E142 neutron data [2], SLAC E154 neutron data [6], SMC combined proton data [10], the SMC deuteron data [9] which are combined data from the 1992, 1994 [7] and 1995 runs, HERMES neutron data [11] and the final SLAC E143 results [5] on g_1^p/F_1^p and g_1^d/F_1^d . The data used (354 experimental points) cover the following kinematic region:

$$0.004 < x < 0.75, \quad 1 < Q^2 < 72 \text{ GeV}^2. \quad (36)$$

As mentioned in the Introduction, in contrast to the other analyses, we fit all possible (x, Q^2) data rather than ones averaged over Q^2 within each x -bin. We denote this combined fit to the (x, Q^2) data on A_1^N presented by E142, E143 and SMC collaborations and the averaged A_1^N data given by EMC, E154 and HERMES as Fit A. Since for most of these data (E142, SMC) the systematic errors are not published, in Fit A only statistical errors are taken into account. The results of the fit to the averaged A_1^N data alone (118 experimental data points) given by all the collaborations mentioned above are also presented (Fit B). In this case the total (statistical and systematic) errors are included in the analysis. "Higher twist" corrections are not included in the present study. As already discussed above, in the approach used their effect is expected to be negligible.

The numerical results of the fits ($\lambda = 1$) are listed in Table 1. Note that $\eta_{\bar{s}} = \eta_S/6$ in the SU(3) symmetry case. The dependence of the results on the flavour decomposition of the sea will be discussed below in detail.

It follows from our analysis that the value of a_g can not be well determined, i.e. the existing data do not constrain the behaviour of the polarized gluon density at small x . For that reason the fits to the data were performed at different fixed values of a_g in the range: $0 \leq a_g \leq 1$. In Fit A the change of χ^2/DOF value from $\chi^2/DOF(a_g = 0) = 0.917$ to $\chi^2/DOF(a_g = 1) = 0.910$ is negligible. The same conclusion is true for the fits to the average A_1 data. In Table 1 we present the results of the fits corresponding to $a_g = 0.6$.

In Fig. 1 the SLAC/E143 and SMC data on A_1^p and A_1^d vs Q^2 for different x -bins are compared to our best Fit A. The NLO results for the averaged asymmetries A_1^N

(Fit B) are shown in Fig. 2. It is seen from the values of χ^2/DOF and Figs. 1 and 2 that the NLO QCD predictions are in a very good agreement with the presently available data on A_1^N , as well as with the corresponding $g_1^N(x, Q^2)$ data (see Figs. 6a and b). We would like to draw special attention to the excellent fit to the E154 neutron data (see Fig. 2c), the most accurate polarized DIS data at present ($\chi^2 = 1.6$ for 11 experimental data points).

Table 1. Results of the NLO QCD fits to the world A_1^N data ($Q_0^2 = 1 \text{ GeV}^2$). For Fit A errors are statistical, for Fit B, total. $a_g = 0.6$ (fixed).

Parameters	Fit A	Fit B
DOF	354 - 5	118 - 5
χ^2	318.4	86.1
χ^2/DOF	0.912	0.762
a_u	0.250 ± 0.023	0.255 ± 0.028
a_d	0.231 ± 0.088	0.148 ± 0.113
a_S	0.576 ± 0.152	0.817 ± 0.223
$\eta_{\bar{s}}$	-0.054 ± 0.012	-0.049 ± 0.005
η_g	0.34 ± 0.24	0.82 ± 0.32
$a_0 = \Delta\Sigma(1)_{\overline{MS}}$	0.253 ± 0.079	0.287 ± 0.041
$\Delta\Sigma(1)_{AB}$	0.332 ± 0.096	0.476 ± 0.084

One can see from Fig. 1 that the accuracy and the presently measured kinematic region of the data do not allow a definite conclusion about the scaling violations in $A_1^N(x, Q^2)$. It is obvious that more precise data and an extension of the measured range to smaller x and larger Q^2 are needed to answer the question about the Q^2 dependence of virtual photon spin asymmetry A_1^N .

The extracted valence, strange and gluon polarized distributions at $Q^2 = 1 \text{ GeV}^2$ are shown in Fig. 3a: Fit A (solid curves) and Fit B (dashed curves). Except for the gluon these two sets of densities coincide almost exactly in the measured x -region. The polarized gluon densities extracted in Fit A and Fit B are a good illustration of how large the uncertainty is in determining the gluon density from the present data. Although the values of their first moments η_g are in agreement within two standard deviations, their central values differ by a factor of more than two. (Note that in Fit A and B the same form of the initial parton densities has been used.)

In Fig. 3b and Fig. 4 the nonsinglet combinations $x\Delta q_3$, $x\Delta q_8$ and their ratio $\Delta q_3/\Delta q_8$ are shown, respectively. The ratio $\Delta q_3/\Delta q_8$ is shown at $Q^2 = 1 \text{ GeV}^2$, but it does not change with Q^2 because the same evolution holds for both $x\Delta q_3$ and $x\Delta q_8$. We find a significant deviation from the approximation (13) used in [16] by Altarelli et al. Note that the Q^2 evolution of the nonsinglets is the same in all the schemes discussed in Section 2.4.

Let us now examine how the assumption (10) about the flavour decomposition of the sea influences our results. As pointed out in Section 2.2 the strange quark density, and in particular, its first moment $\Delta\bar{s}(1, Q_0^2)$ should not change as λ is varied. The results of the fits to the averaged A_1^N data (Fit B) using different values of λ are presented in Table 2.

Table 2. The results for the first moments of the polarized distributions at $Q^2 = 1 \text{ GeV}^2$ using the assumption (10) about the flavour decomposition of the sea.

λ	χ^2	$-\eta_{\bar{s}}$	η_g	η_u	$-\eta_d$
0.5	85.97	0.049 ± 0.004	0.78 ± 0.31	0.869 ± 0.013	0.388 ± 0.013
1.0	86.11	0.049 ± 0.005	0.82 ± 0.32	0.918 ± 0.013	0.339 ± 0.013
2.0	86.08	0.050 ± 0.007	0.86 ± 0.34	1.018 ± 0.019	0.239 ± 0.019
3.0	86.12	0.048 ± 0.004	0.93 ± 0.35	1.110 ± 0.020	0.147 ± 0.020

It is clear from the table that χ^2 and the central values of $\eta_{\bar{s}} \equiv \Delta\bar{s}(1, Q_0^2)$ and $\eta_g \equiv \Delta G(1, Q_0^2)$ practically do not change as λ varies. We regard this fact as a very good test of the stability of our analysis. We thus conclude, somewhat in disagreement with Ref. [16] that the separation into valence and sea contributions need not introduce biases into the fit provided sufficient care is taken. Of course, we have also demonstrated very clearly that the Δu_v and Δd_v valence quark densities are sensitive to the assumptions about the sea. This dependence is shown in Fig. 5.

What follows from our analysis is that one can use for input distributions a parametrization in terms of valence and sea quarks. With a correct fitting procedure the strange sea (or singlet, see (11)) and gluon distributions defined from the inclusive data do not depend on the assumption about the sea and therefore, one can use them to test the remarkable relation (19). On the contrary, as emphasized in Section 2.2, electromagnetic DIS does not fix the valence quark densities, which are sensitive to the

assumption about the sea. This implies that is somewhat meaningless to claim [26] that "the present semi-inclusive data alone fail to define a Δd_v distribution consistent with those extracted from inclusive data".

In Table 1 we also present our results for the first moments of the polarized gluon and singlet quark densities in the \overline{MS} (determined from the fit) and AB (calculated by Eq. (17)) schemes. The value of η_g (Fit B)

$$\eta_g \equiv \Delta G(1, 1 \text{ GeV}^2)_{\overline{MS}} = \Delta G(1, 1 \text{ GeV}^2)_{AB} = 0.82 \pm 0.32 \quad (37)$$

is in a good agreement with the one obtained in Fit A of Ref. [16]:

$$\Delta G(1, 1 \text{ GeV}^2)_{AB} = 0.95 \pm 0.18 \quad (38)$$

using almost the same data.

Our result for $\Delta\Sigma(1)_{AB}$

$$\Delta\Sigma(1)_{AB} = 0.476 \pm 0.084 \quad (39)$$

is in agreement within two standard deviations with its constituent value 0.6 [40] and, within errors, coincides with the value determined in [16]

$$\Delta\Sigma(1)_{AB} = 0.405 \pm 0.032 . \quad (40)$$

Finally, let us turn to the first moments $\Gamma_1^N(Q^2)$ of the spin structure function $g_1^N(x, Q^2)$. Using our results of the fits for the input polarized parton densities these quantities have been calculated for different values of Q^2 using Eq. (29) for $n = 1$. The results are presented in Table 3.

Table 3. Determination of the first moments $\Gamma_1^N(Q^2)$ of $g_1^N(x, Q^2)$ using the results of our NLO QCD fits to the world A_1^N data.

	Fit A	Fit B
$\Gamma_1^p(5 \text{ GeV}^2)$	0.134	0.138
$\Gamma_1^n(5 \text{ GeV}^2)$	- 0.056	- 0.053
$\Gamma_1^d(5 \text{ GeV}^2)$	0.036	0.039
$\Gamma_1^p(10 \text{ GeV}^2)$	0.136	0.139
$\Gamma_1^n(10 \text{ GeV}^2)$	- 0.057	- 0.054
$\Gamma_1^d(10 \text{ GeV}^2)$	0.036	0.039

The values of the first moments of the polarized parton densities and therefore, the corresponding values of the first moments of g_1^N are very sensitive to the assumed small x -behavior of the input parton densities (see e.g. [6, 10]). Parton densities which give the same results for the physical quantities in the *measured* x region can lead to rather different behaviour at very small x . The dependence of the the moments of the physical quantities in polarized DIS on different assumptions about the small x behaviour of the input parton densities has been studied in detail in [16].

The simple Regge behaviour of the unpolarized and polarized structure functions as $x \rightarrow 0$, which was for many years a guiding principle in our choice of the starting ansatz for the parton densities, differs from that predicted in QCD [41, 42]. Moreover, the unpolarized DIS experiments at HERA have shown that the simple Regge extrapolation of the structure functions at small x is not valid at large Q^2 . There is an indication [6] that this is also true in the polarized case. The question of the small x behaviour in the polarized case remains an open one and is a serious challenge to both experiment and theory.

For illustration we compare our predictions for $\Gamma_1^p(10 \text{ GeV}^2)$ and $\Gamma_1^n(5 \text{ GeV}^2)$

$$\begin{aligned}\Gamma_1^p(10 \text{ GeV}^2) &= \{0.136 \text{ (Fit A)}, 0.139 \text{ (Fit B)}\} , \\ \Gamma_1^n(5 \text{ GeV}^2) &= \{-0.057 \text{ (Fit A)}, -0.054 \text{ (Fit B)}\}\end{aligned}\quad (41)$$

with their "experimental" values [10] and [17]

$$\Gamma_1^p(10 \text{ GeV}^2) = 0.130 \pm 0.006(\text{stat}) \pm 0.008(\text{syst}) \pm 0.014(\text{evol}) , \quad (42)$$

$$\Gamma_1^n(5 \text{ GeV}^2) = -0.058 \pm 0.004(\text{stat}) \pm 0.007(\text{syst}) \pm 0.007(\text{evol}) , \quad (43)$$

the latter chosen because the moments have been determined by extrapolating the polarized structure functions into the unmeasured x region using QCD. It is seen from Eqs. (41)-(43) that our predictions for Γ_1^p and Γ_1^n are in a good agreement with their "experimental" values.

5. Conclusion

We have performed a next-to leading order QCD analysis (\overline{MS} scheme) of the world data on inclusive polarized deep inelastic lepton-nucleon scattering. The QCD predictions have been confronted with the data on the virtual photon-nucleon asymmetry $A_1^N(x, Q^2)$, rather than with the polarized structure function $g_1^N(x, Q^2)$, in order to minimize the higher twist effects. In this paper, for the first time, is utilized the full world data set on A_1^N with its detailed binning in (x, Q^2) . Using the simple

parametrization (30) (with only 5 free parameters) for the input polarized parton densities it was demonstrated that the polarized DIS data are in an excellent agreement with the pQCD predictions for $A_1^N(x, Q^2)$ and the spin-dependent structure function $g_1^N(x, Q^2)$. However, the accuracy and the presently measured kinematic region of the data do not allow a definite conclusion about scaling violations in $A_1^N(x, Q^2)$.

We have studied the consequences of different simplifying assumptions, usually made in recent analyses to aid the extraction of the polarized parton densities from the data. It was shown that whereas the valence quark densities determined from inclusive polarized DIS data, are sensitive to the assumptions about the flavour decomposition of the sea, the extracted strange sea and gluon densities in our analysis do *not* depend on such an assumption and can therefore be used to test the remarkable relation (19). We have found a significant deviation from the approximation (13) used in Ref. [16] that the nonsinglet quark distributions $\Delta q_3(x, Q^2)$ and $\Delta q_8(x, Q^2)$ have the same shape at fixed Q^2 .

Although the quality of the data has significantly improved via the recent experiments of the SLAC/E154 Collaboration and the final SMC results on A_1^p , the uncertainty in determining the polarized gluon density is still very large.

Despite the great progress of the past few years it is clear that in order to test precisely the spin properties of QCD, more accurate inclusive DIS polarized data and an extension of the measured range to smaller x and larger Q^2 are needed. We hope the current DIS experiments at HERA will help in clarifying the situation. In addition, semi-inclusive and charged current data will be very important for a precise determination of the polarized parton densities and especially, for an accurate flavour decomposition of the polarized quark sea. There is some progress in this direction [26]. Finally, a direct measurement of $\Delta G(x, Q^2)$ in processes such as J/ψ production in lepton-hadron scattering with a polarized beam will answer the important question about the magnitude of the first moment of the gluon density $\Delta G(x, Q^2)$.

Acknowledgments

We are grateful to O. V. Teryaev for useful discussions and remarks.

This research was partly supported by a UK Royal Society Collaborative Grant, by the Russian Fund for Fundamental Research Grant No 96-02-17435a and by the Bulgarian Science Foundation under Contract Ph 510.

References

- [1] EMC, J. Ashman et al., *Phys. Lett.* **B206**, 364 (1988);
Nucl. Phys. **B328**, 1 (1989).
- [2] SLAC E142 Collaboration, P. L. Anthony et al., *Phys. Rev.* **D54**, 6620 (1996).
- [3] SLAC E143 Collaboration, K. Abe et al., *Phys. Rev. Lett.* **74**, 346 (1995);
Phys. Rev. Lett. **75**, 25 (1995).
- [4] SLAC E143 Collaboration, K. Abe et al., *Phys. Lett.* **B364**, 61 (1995).
- [5] SLAC E143 Collaboration, K. Abe et al., Preprint SLAC-PUB-7753, Feb 1998,
e-Print Archive:hep-ph/9802357.
- [6] SLAC/E154 Collaboration, K. Abe et al., *Phys. Rev. Lett.* **79**, 26 (1997).
- [7] SMC, D. Adeva et al., *Phys. Lett.* **B302**, 533 (1993);
D. Adams et al., *Phys. Lett.* **B357**, 248 (1995).
- [8] SMC, D. Adams et al., *Phys. Lett.* **B329**, 399 (1994),
erratum *ibid* **B339** 332 (1994); *Phys. Rev.* **D56**, 5330 (1997).
- [9] SMC, D. Adams et al., *Phys. Lett.* **B396**, 338 (1997).
- [10] SMC, D. Adeva et al., *Phys. Lett.* **B412**, 414 (1997).
- [11] HERMES Collaboration, K. Ackerstaff et al., *Phys. Lett.* **B404**, 383 (1997).
- [12] SMC, D. Adams et al., *Phys. Lett.* **B336**, 125 (1994);
SLAC E143 Collaboration, K. Abe et al., *Phys. Rev. Lett.* **76**, 587 (1996);
SLAC/E154 Collaboration, K. Abe et al., *Phys. Lett.* **B404**, 377 (1997).
- [13] T. Gehrmann and W. J. Stirling, *Phys. Rev.* **D53**, 6100 (1996).
- [14] M. Glück, E. Reya, M. Stratmann and W. Vogelsang, *Phys. Rev.* **D53**,
4775 (1996).
- [15] R. D. Ball, S. Forte and G. Ridolfi, *Phys. Lett.* **B378**, 255 (1996).

- [16] G. Altarelli, R. D. Ball, S. Forte and G. Ridolfi, *Nucl. Phys.* **B496**, 337 (1997);
Acta Phys. Polon. **B29**, 1145 (1998), e-Print Archive:hep-ph/9803237.
- [17] SLAC/E154 Collaboration, K. Abe et al., *Phys. Lett.* **B405**, 180 (1997).
- [18] E. Leader, A. V. Sidorov and D. B. Stamenov,
e-Print Archive:hep-ph/9708335 (to be published in IJMPA).
- [19] M. Stratmann, Preprint DO-TH 97/22, October 1997,
e-Print Archive:hep-ph/9710379.
- [20] A. De Roeck et al., Preprint DESY 97-249, e-Print Archive:hep-ph/9801300.
- [21] C. Bourrely, F. Buccella, O. Pisanti, P. Santorelli and J. Soffer,
Preprint CPT-97/P 3578, e-Print Archive:hep-ph/9803229.
- [22] R. Mertig and W. L. van Neerven, *Z. Phys.* **C70**, 637 (1996);
W. Vogelsang, *Phys. Rev.* **D54**, 2023 (1996).
- [23] A. D. Martin, R. G. Roberts, W. J. Stirling and R. S. Torn,
Preprint RAL-TR-98-029, e-Print Archive:hep-ph/9803445.
- [24] See for example:W. J. Stirling, Preprint DTP-97-80, Jun 1997,
e-Print Archive:hep-ph/9709429.
- [25] EMC, J. Ashman et al., *Nucl. Phys.* **B328**, 1 (1989);
SMC Collaboration, B. Adeva et al., *Phys. Lett.* **B369**, 93 (1996);
B420, 180 (1998).
- [26] D. de Florian, O. A. Sampayo and R. Sassot, *Phys. Rev.* **D57**, 5803 (1998).
- [27] A. V. Efremov and O. V. Teryaev, Dubna report E2-88-287, 1988 (published in
the Proceedings of the Int. Hadron Symposium, Bechyne, Czechoslovakia, 1988,
eds. J. Fischer et al. (Czech Academy of Science, Prague, 1989), p. 302);
G. Altarelli and G. G. Ross, *Phys. Lett.* **B212**, 381 (1988).
- [28] R. D. Carlitz, J. C. Collins and A.H. Mueller, *Phys. Lett.* **B214**, 229 (1988).
- [29] S. Adler and W. Bardeen, *Phys. Rev.* **182**, 1517 (1969).
- [30] E. Leader and M. Anselmino, *Z. Phys.* **C41**, 239 (1988).
- [31] E. B. Zijlstra and W. L. van Neerven, *Nucl. Phys.* **B147**, 61 (1994).

- [32] M. Anselmino, A. V. Efremov and E. Leader, *Phys. Rep.* **261**, 1 (1995).
- [33] D. Müller and O. V. Teryaev, *Phys. Rev.* **D56**, 2607 (1997).
- [34] Hai-Yang Cheng, e-Print Archive:hep-ph/9712473.
- [35] E. Leader, A. V. Sidorov and D. B. Stamenov, a paper in preparation.
- [36] M. Glück, E. Reya and A. Vogt, *Z. Phys.* **C67**, 433 (1995).
- [37] G. Parisi and N. Surlas, *Nucl. Phys.* **B151**, 421 (1979);
I. S. Barker, C. B. Langensiepen and G. Shaw, *Nucl. Phys.* **B186**, 61 (1981).
- [38] V. G. Krivokhizhin et al., *Z. Phys.* **C36**, 51 (1987); *ibid* **C48**, 347 (1990).
- [39] Particle Data Group, L. Montanet et al., *Phys. Rev.* **D50**, 1173 (1994);
F. E. Close and R. G. Roberts, *Phys. Lett.* **B313**, 165 (1993).
- [40] R. L. Jaffe and A. Manohar, *Nucl. Phys.* **B337**, 509 (1990).
- [41] R. D. Ball, S. Forte and G. Ridolfi, *Nucl. Phys.* **B444**, 287 (1995).
- [42] J. Batrels, B. I. Ermolaev and M. G. Ryskin, *Z. Phys.* **C70**, 273 (1996);
C72, 627 (1996).

Figure Captions

Fig. 1a-1b. A_1^p and A_1^d vs Q^2 for different x -bins for the proton E143 [4] and SMC data [10] and for deuteron E143 [4] and SMC data [9]. Only statistical errors are shown. The solid curves correspond to Fit A described in the text. The E143 data on g_1/F_1 are multiplied by the kinematic factor $(1 + \gamma^2)$.

Fig. 2a-2c. Comparison of our NLO results (Fit B) for averaged $A_1^N(x, Q^2)$ with the experimental data at the measured x and Q^2 values. Errors bars represent the total error.

Fig. 3a-3b. Next-to-leading order input polarized parton distributions at $Q^2 = 1 \text{ GeV}^2$ ($\lambda = 1$). Solid and dashed curves in Fig. 3a correspond to Fit A and Fit B, respectively.

Fig. 4. Comparison between our result (solid curve) for the ratio $\Delta q_3(x)/\Delta q_8(x)$ and approximation (13) used in Ref. [16] (dashed line).

Fig. 5. Polarized valence quark densities at $Q^2 = 1 \text{ GeV}^2$ for different values of λ (see Eq. (10)). The solid curves correspond to an $SU(3)$ flavour symmetric sea ($\lambda = 1$).

Fig. 6a-6b. Comparison of our NLO results for $g_1^N(x, Q^2)$ (6a) and $xg_1^N(x, Q^2)$ (6b) with SMC [9, 10] and SLAC/E154 data [6] at the measured values of Q^2 . Error bars represent the total error.

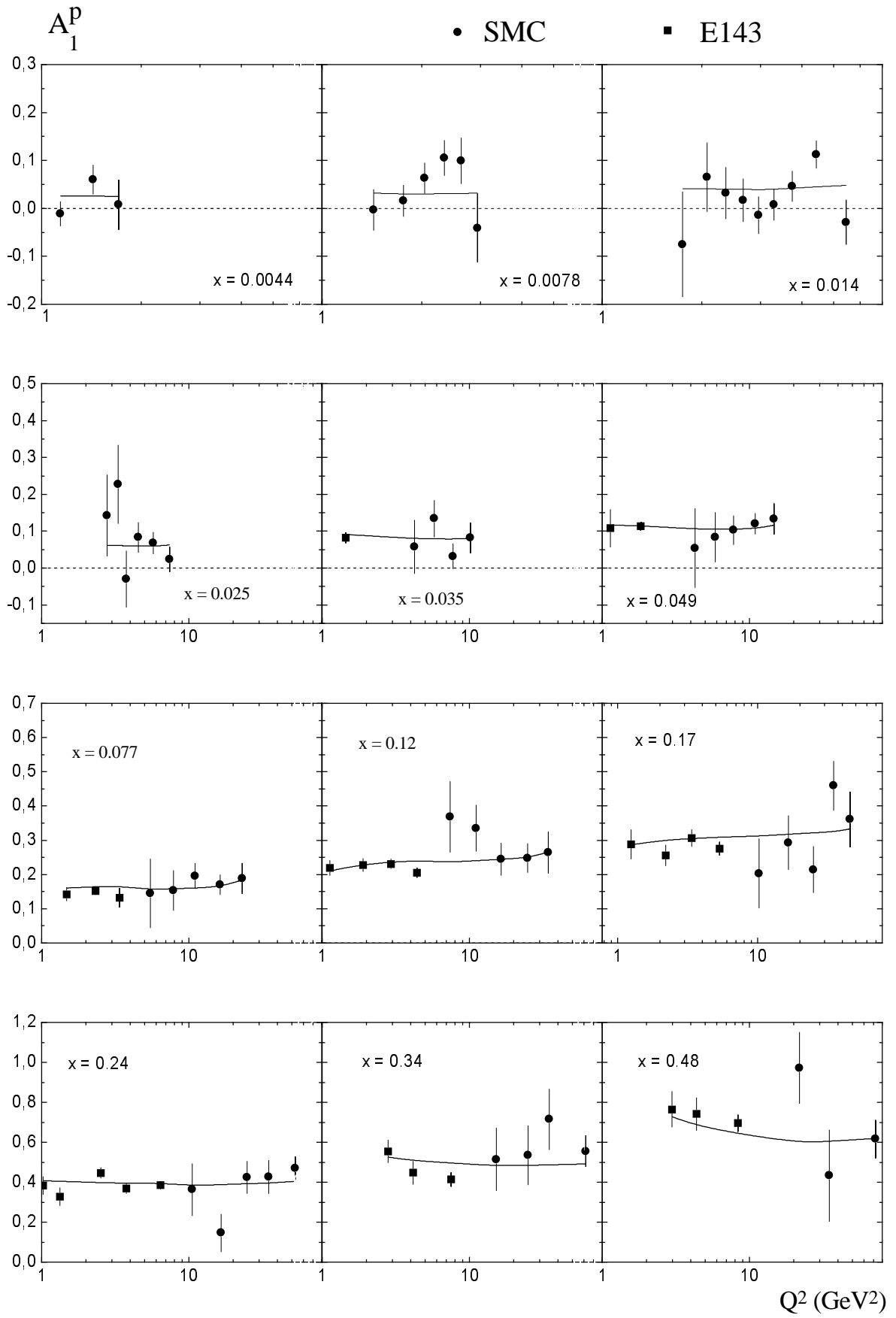


Fig. 1a

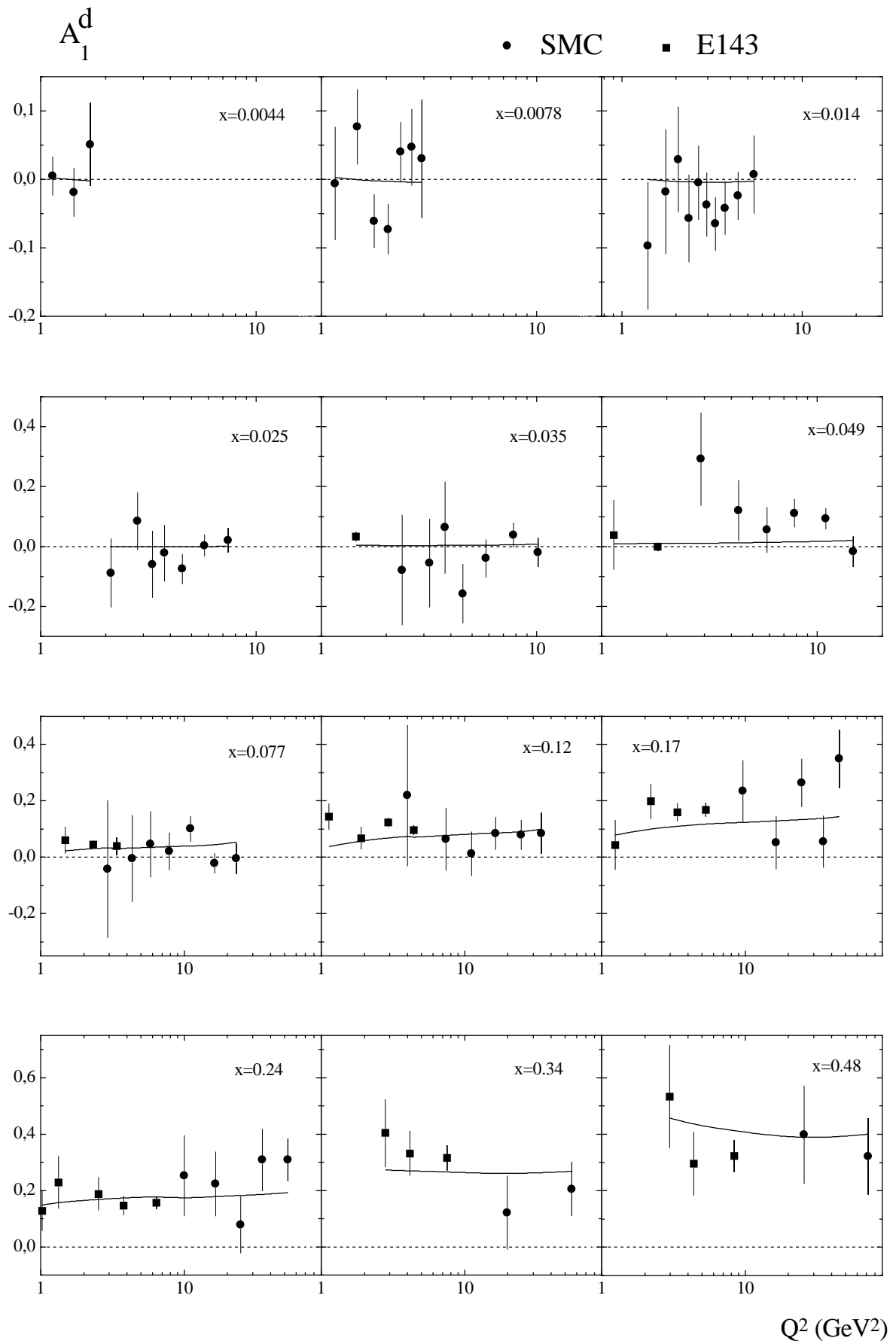


Fig. 1b

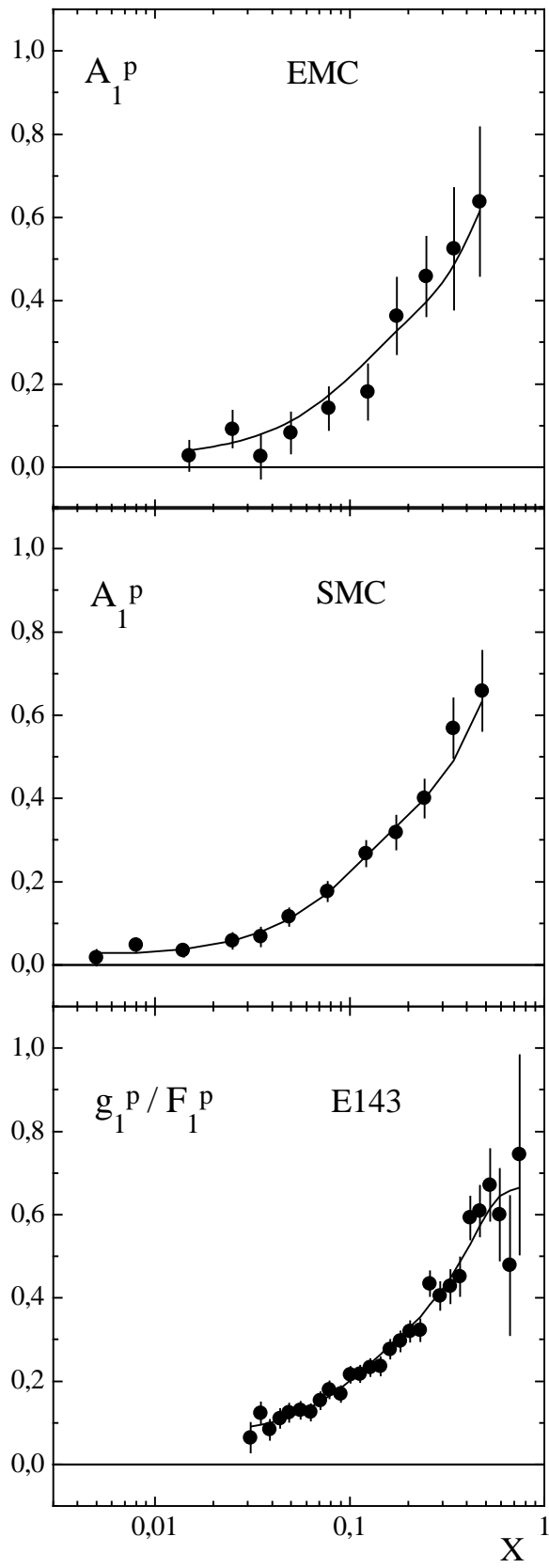


Fig. 2a

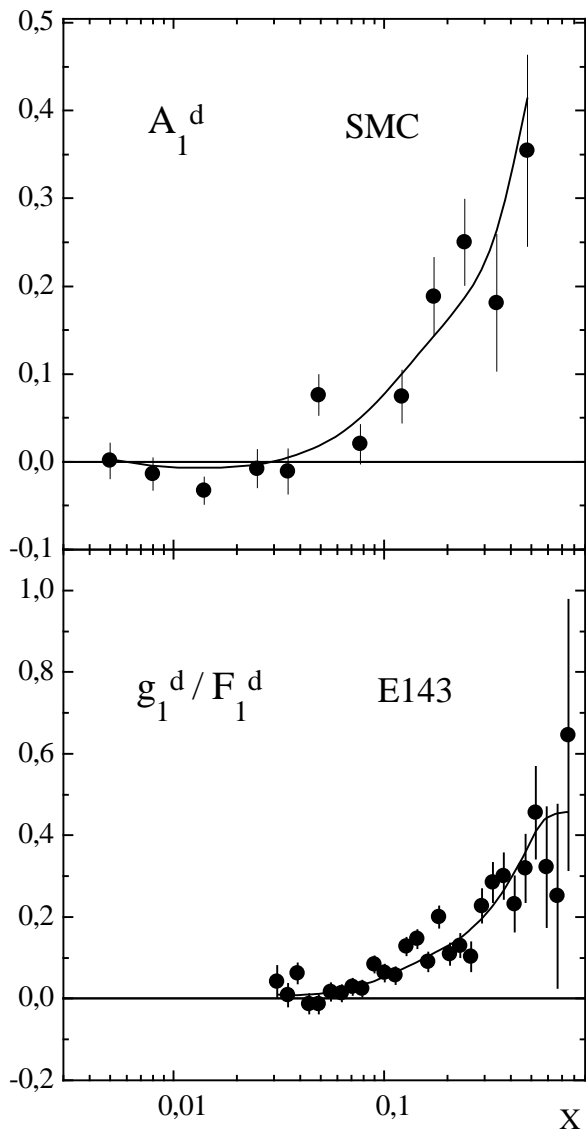


Fig. 2b

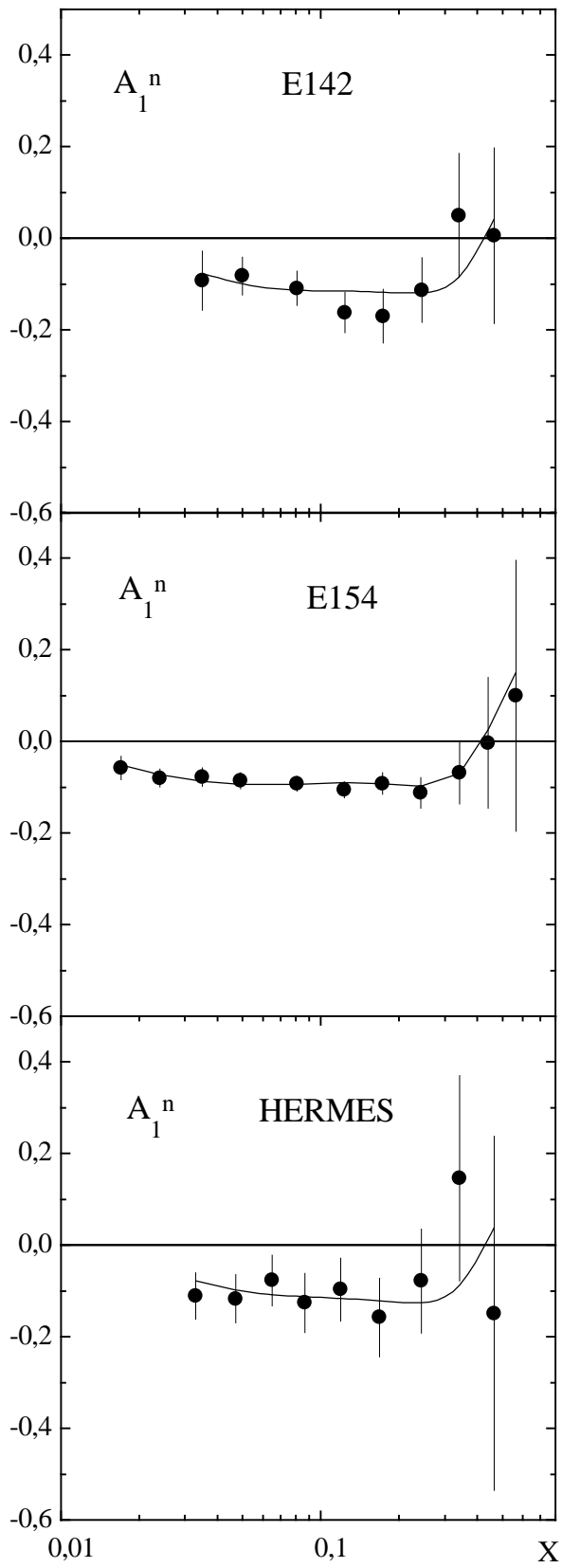


Fig. 2c

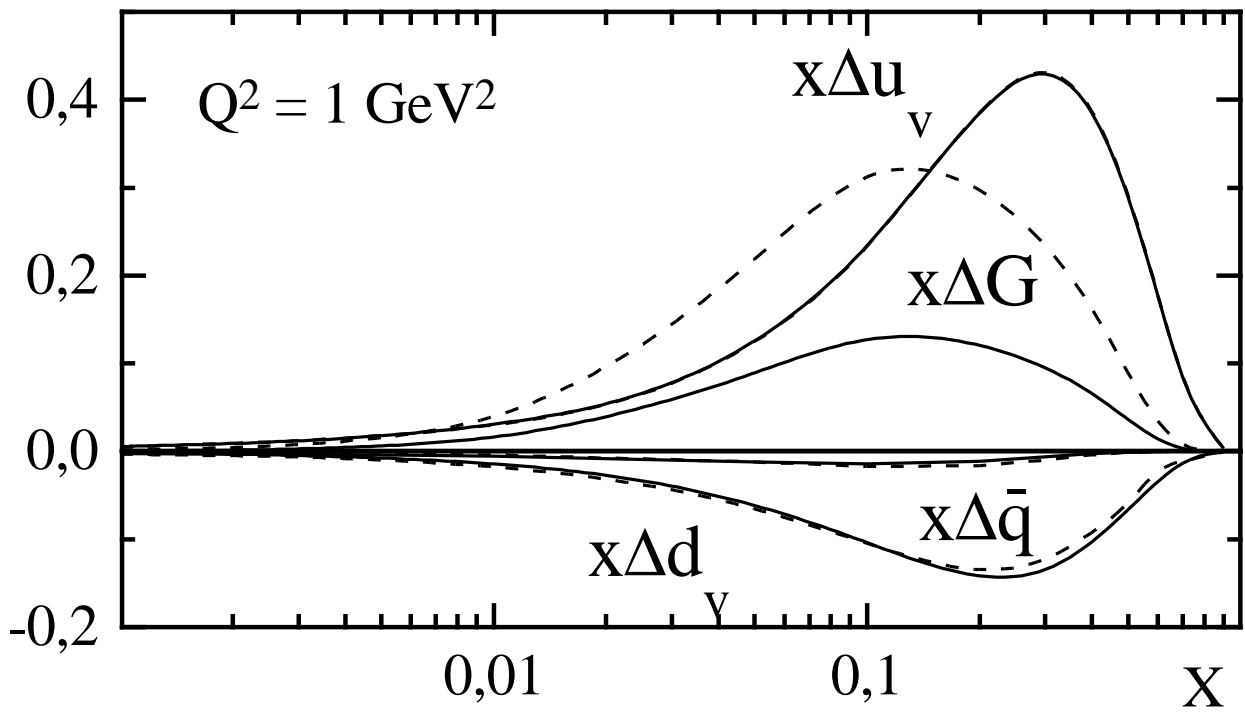


Fig. 3a

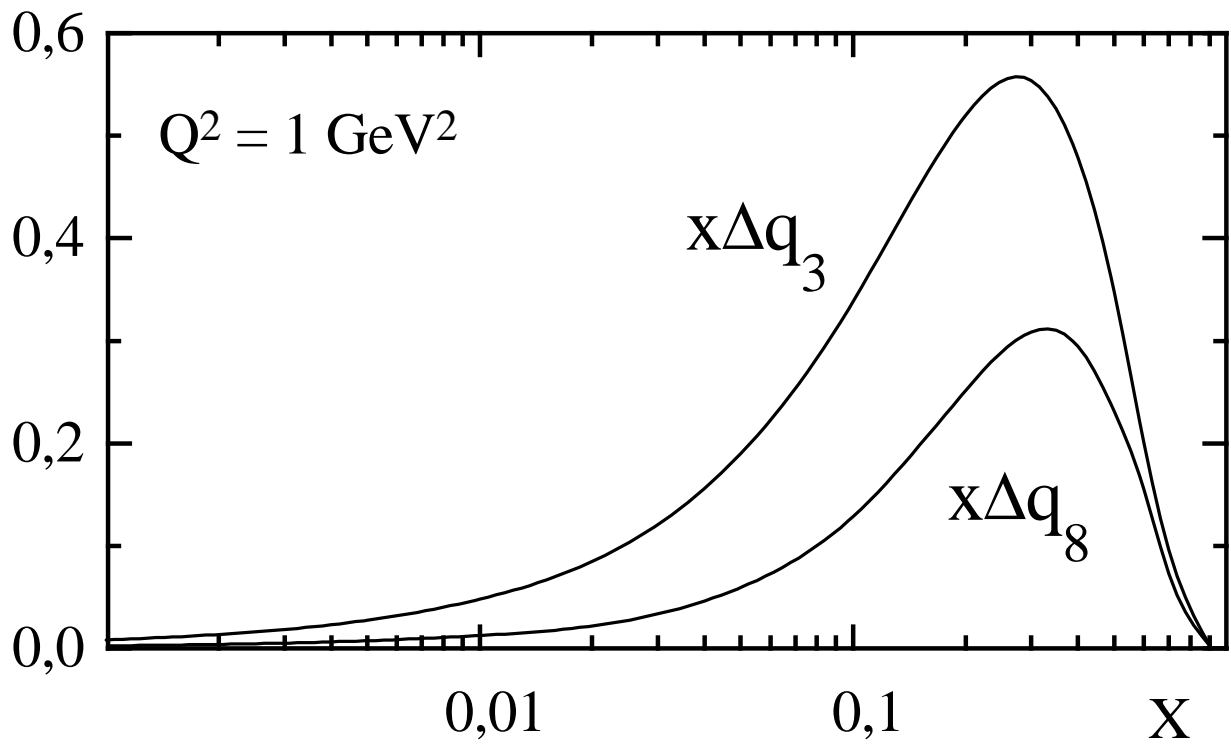


Fig. 3b

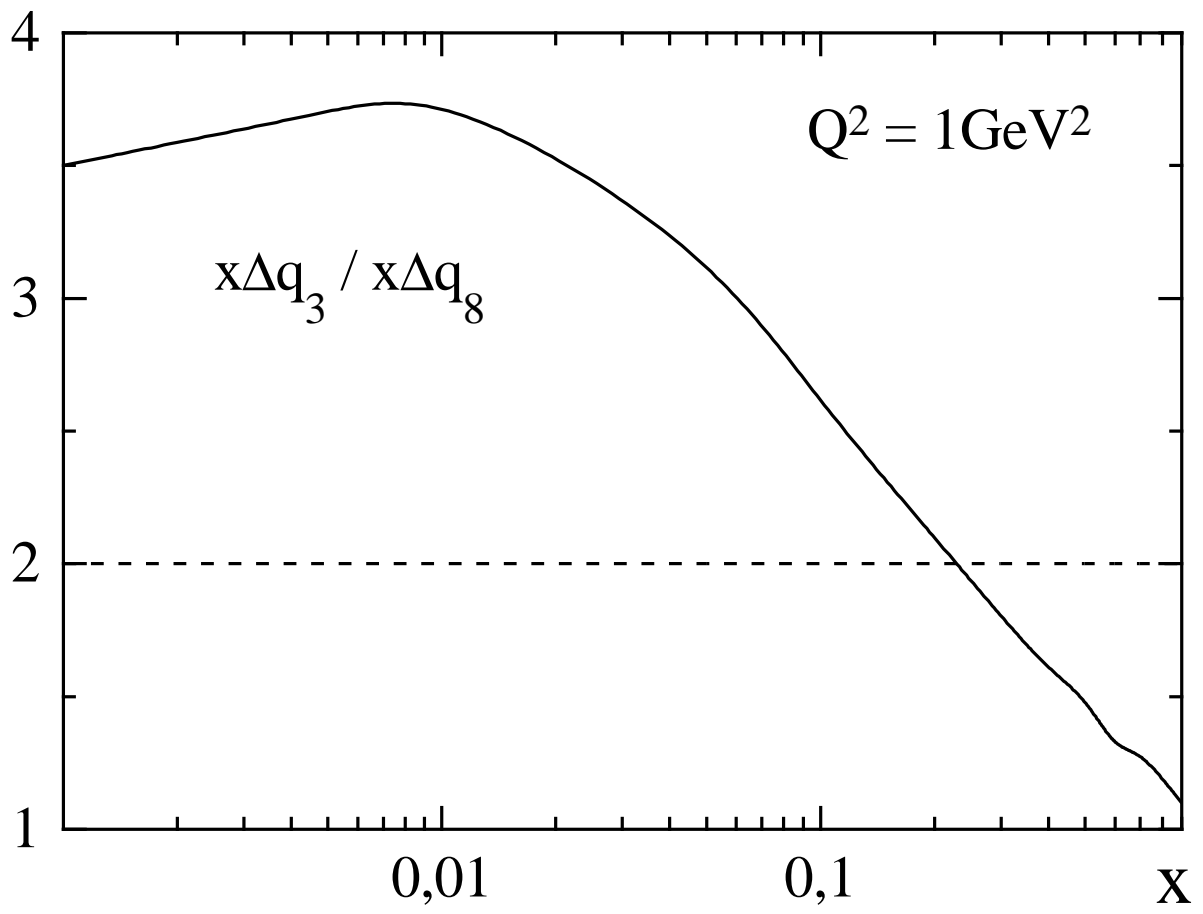


Fig. 4

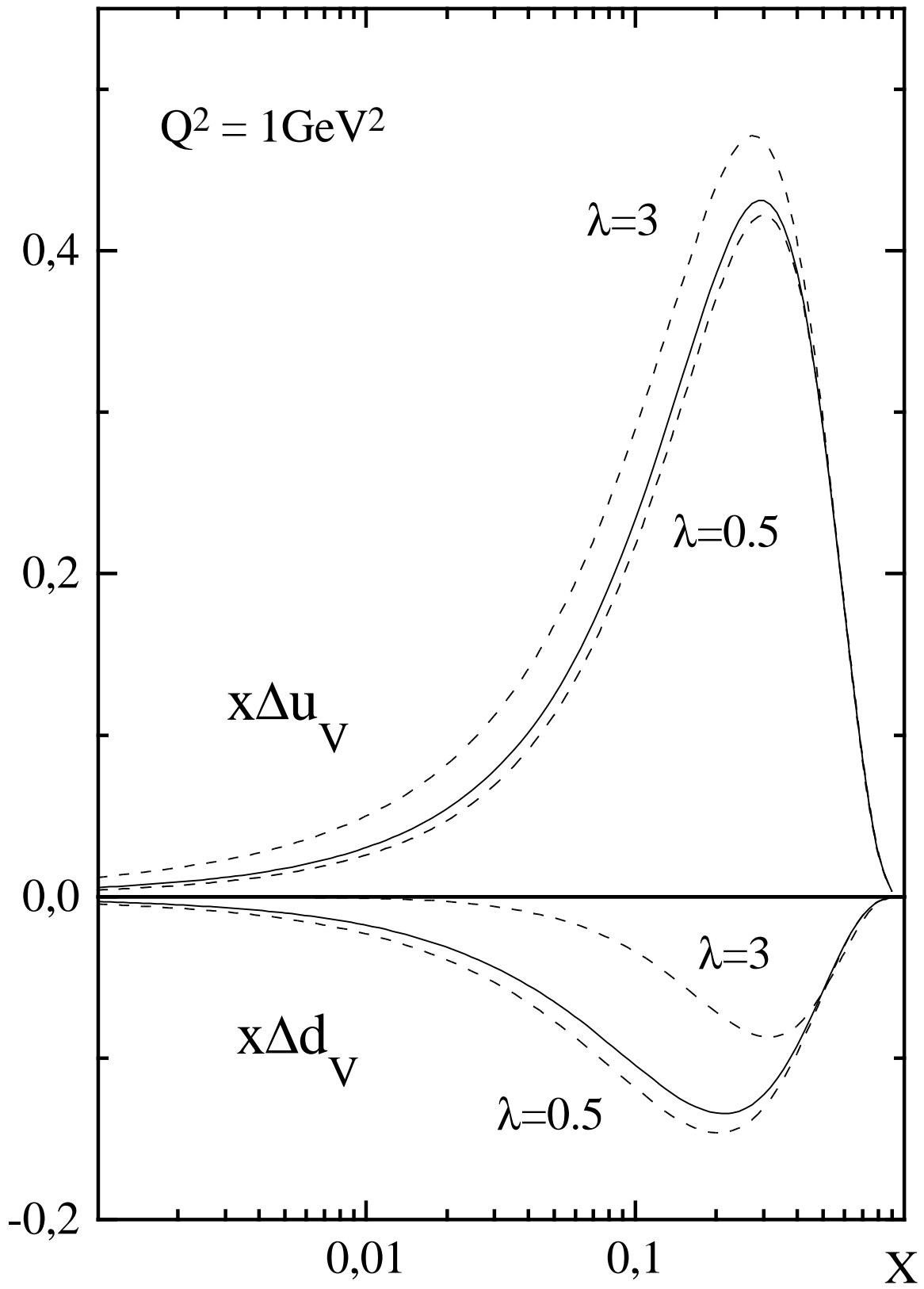


Fig. 5

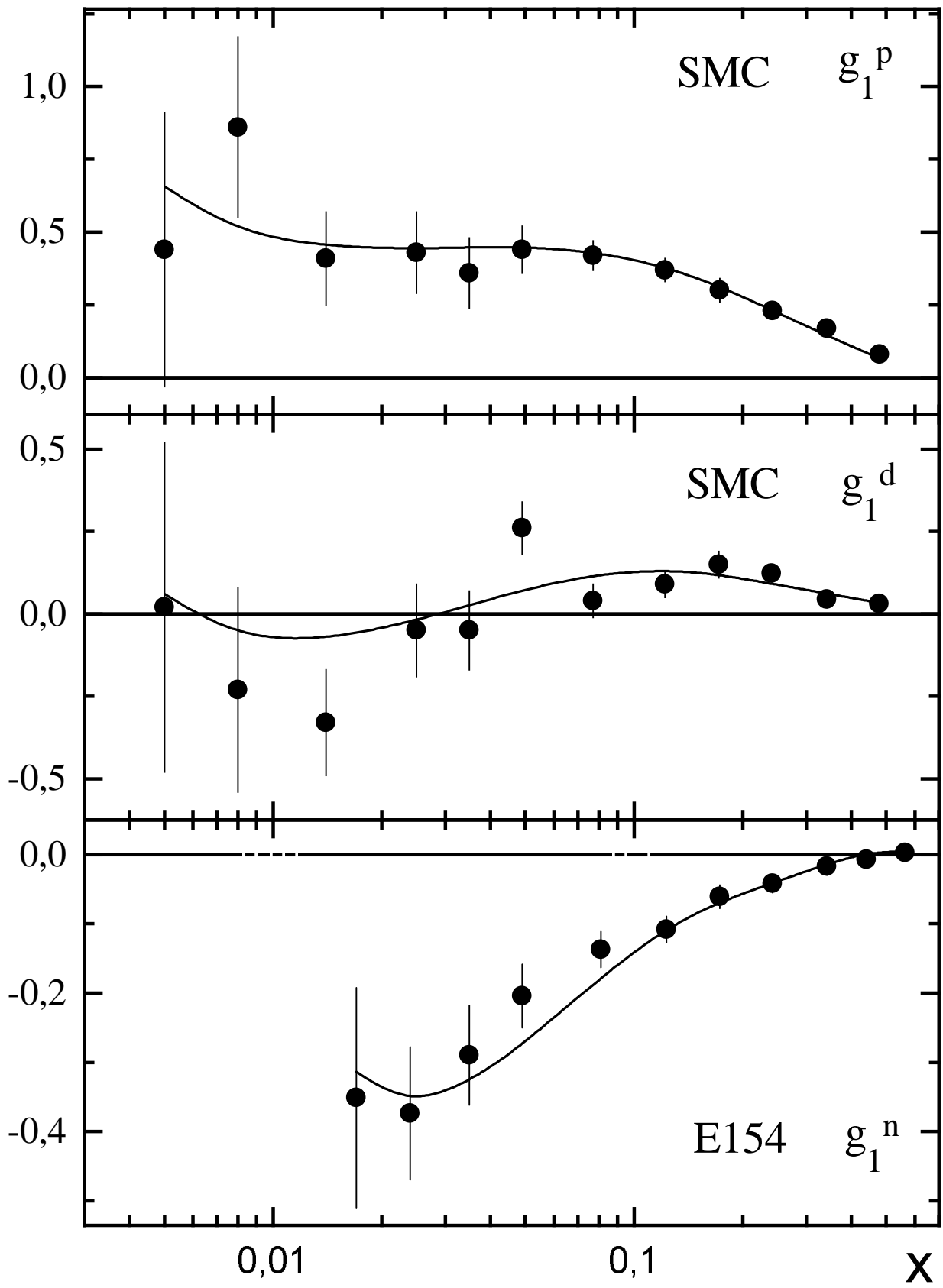


Fig. 6a

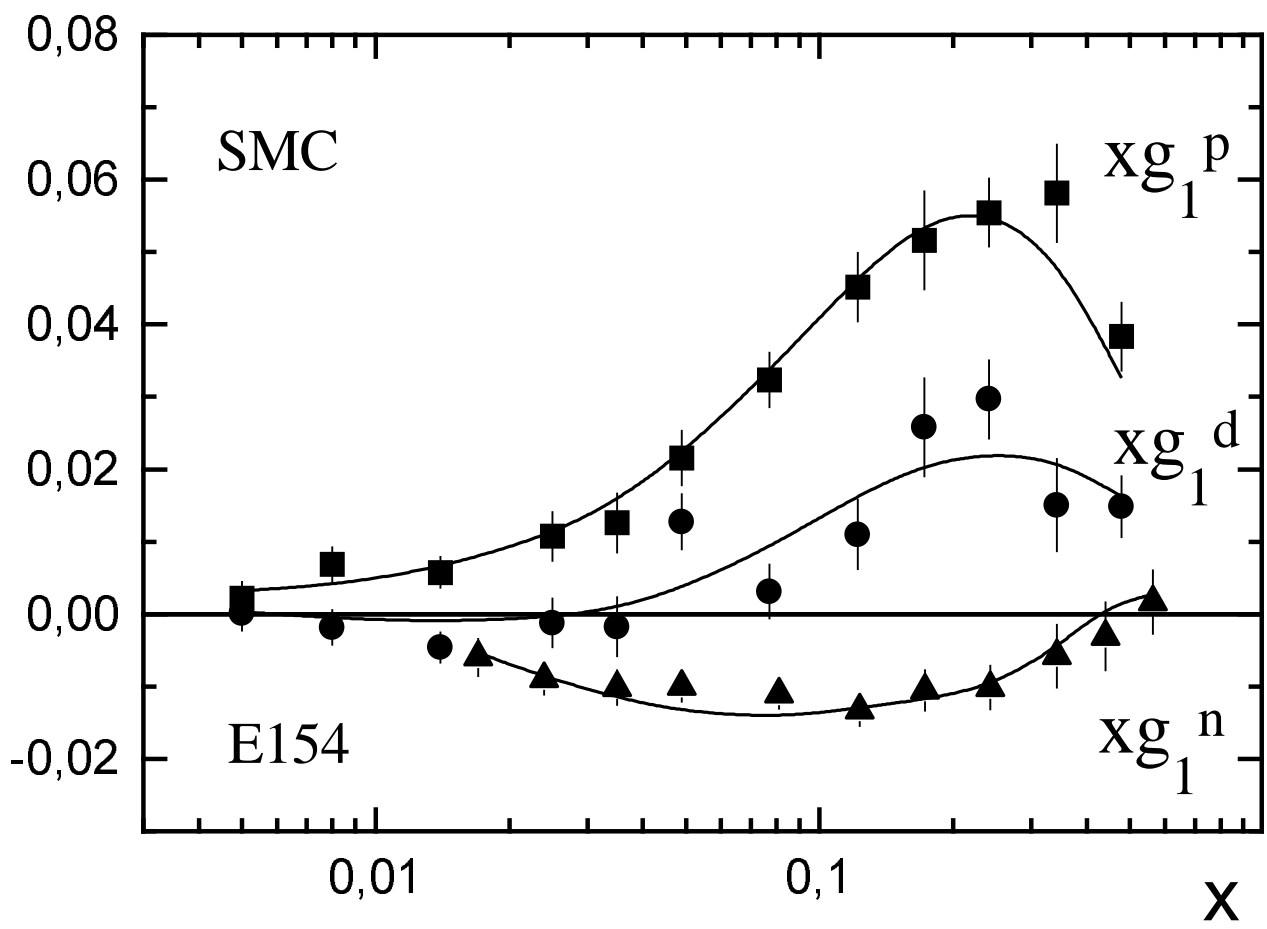


Fig. 6b